Naval Research Laboratory

Washington, DC 20375-5320

NRL/MR/6410--00-8428

Advanced Simulation Tool for Improved Damage Assessment 1) A Multiblock Technique for Simulating Fire and Smoke Spread in Large Complex Enclosures

KULDEEP PRASAD*
GOPAL PATNAIK
K. KAILASANATH

Center for Reactive Flow and Dynamical Systems
Laboratory for Computational Physics and Fluid Dynamics

**Science Applications International Corporation, VA*

February 21, 2000

REPORT DOCUMENTATION PAGE

Form Approved
OMB No. 0704-0188

1. AGENCY USE ONLY (*Leave Blank*)	2. REPORT DATE	3. REPORT TYPE AND DATES COVERED
	February 21, 2000	NRL Memorandum Report

4. TITLE AND SUBTITLE

Advanced Simulation Tool for Improved Damage Assessment — 1) A Multiblock Technique for Simulating Fire and Smoke Spread in Large Complex Enclosures

5. FUNDING NUMBERS

PE — 62121N

6. AUTHOR(S)

Kuldeep Prasad*, Gopal Patnaik, and K. Kailasanath

7. PERFORMING ORGANIZATION NAME(S) AND ADDRESS(ES)

Naval Research Laboratory
Washington, DC 20375-5320

8. PERFORMING ORGANIZATION REPORT NUMBER

NRL/MR/6410--00-8428

9. SPONSORING/MONITORING AGENCY NAME(S) AND ADDRESS(ES)

Office of Naval Research
Arlington, VA 22217

10. SPONSORING/MONITORING AGENCY REPORT NUMBER

11. SUPPLEMENTARY NOTES

*Science Applications International Corporation, VA

12a. DISTRIBUTION/AVAILABILITY STATEMENT

Approved for public release; distribution unlimited.

12b. DISTRIBUTION CODE

13. ABSTRACT (*Maximum 200 words*)

Several recent developments in computational techniques have been combined to develop a tool for simulating the reactive flow field inside large complex enclosures. The multiblock technique was adopted to solve the unsteady compressible Navier-Stokes equations inside a large fire compartment. Numerical simulations of a 330 *k*W and a 980 *k*W fire in a single uncluttered compartment have been performed. Peak ceiling jet temperature of 430 °C and 910 °C was computed, for the two fires, respectively. The multiblock approach efficiently grids regions of high heat release with a fine mesh embedded in a coarser mesh covering the larger compartment. It also allows flowfield information to be exchanged with the surrounding air through the doorway. Temperature contours and instantaneous velocity vectors provide a detailed understanding of air entrainment into the fire and the flow of hot gases through the door. Numerical results have been found to compare favorably with experimental data. Computations are also reported for a 1310 *k*W fire in a multi-compartment geometry that replicates the ex-USS Shadwell. Peak temperatures of 320 °C are obtained in this case. Our results predict a continuously evolving flowfield as unsteady vortical structures are generated in the fire plume and convect through the various compartments via the doors and hatches.

14. SUBJECT TERMS

Multiblock technique
Air entrainment
Combustion
Flow field
Fire and smoke spread
Fire simulation
Complex enclosures
Detonation

15. NUMBER OF PAGES

28

16. PRICE CODE

17. SECURITY CLASSIFICATION OF REPORT	18. SECURITY CLASSIFICATION OF THIS PAGE	19. SECURITY CLASSIFICATION OF ABSTRACT	20. LIMITATION OF ABSTRACT
UNCLASSIFIED	UNCLASSIFIED	UNCLASSIFIED	UL

NSN 7540-01-280-5500

Standard Form 298 (Rev. 2-89)
Prescribed by ANSI Std 239-18
298-102

CONTENTS

LIST OF FIGURES

Advanced Simulation Tool for Improved Damage Assessment. 1) A Multiblock Technique for Simulating Fire and Smoke Spread in Large Complex Enclosures

1. INTRODUCTION

Shipboard and submarine fires present a variety of novel problems for firefighters due to the unique nature of the environment. In particular, the enclosed spaces permit heat and smoke to build to levels far in excess of those found in most structural fires. Further aggravating the situation is the high rate of heat transfer through the steel bulkheads and decks, which contributes to rapid fire spread. Firefighting in cluttered machinery spaces has its unique challenges. A computer based model that can quickly and accurately estimate the impact of a fire, and the effectiveness of measures used to control the fire can be a valuable tool for firefighting.

There are two major classes of computer models for analysing fire development in large enclosures. Stochastic or probabilistic models [1] generally treat the fire growth as a series of sequential events or states. Mathematical rules are established to govern the transition from one event to another and probabilities are assigned to each transfer point based on analysis of relevant experimental data and historical fire incidence data. In contrast, deterministic models represent the processes encountered in a compartment fire by mathematical expressions based on physics and chemistry. The most common type of deterministic fire model is the "zone" or "control volume" based model. The zone model [2]- [6] represents the system as a few distinct compartment gas zones resulting from thermal stratification due to buoyancy. The fire is represented as a source of energy and mass, and manifests itself as a plume, which acts as a pump for the mass from the lower zones to the upper zones. Zone models utilize equations employing empirical relationships and constants obtained from experiments. These empirical expressions will break down as the geometries become more complex. Any radical departure by the fire system from the basic concept of the zone model can seriously affect the accuracy and validity of the approach. The building block of the zone model is the conservation equations for the upper and lower gas zones. These equations are developed either by using fundamental equations of energy and mass transport in control volume form as applied to the zones or by using differential equations that represent the conservation laws and integrating them over the zones. The momentum equations are not explicitly used. Information needed to compute velocities and pressures is based on simplifying assumptions and specific applications of momentum principles at vent boundaries of the compartment. Fowkes [2] in his work with Emmons appears to be the first to publish a basis for the zone model approach. Almost simultaneously, computer models based on the zone model approach were produced by Quintiere [3], Pape and Waterman [4] and by Mitler working with Emmons [5]. ASET [7], CFAST [8], FIRST [9] and WPI/FIRE [10] are some of the zone based computer models that are presently being used for studying fires in large enclosures.

Manuscript approved January 18, 2000

The more detailed form of deterministic fire models is the field model [11]- [17]. Field models solve the fundamental equations of mass, momentum and energy in an enclosure that has been divided into much smaller units. Typical field models calculate the velocity and temperature fields, given a prescribed heat source. Some models also calculate gas species and particle concentrations as a function of position and time. In contrast, zone models calculate maximum temperatures or bulk average values predicted at a few select locations within an enclosure. UNDSAFE [11] developed by University of Notre-Dame, BF3D [12] developed by National Institute of Standards and Technology, JASMINE [13] developed by the Fire Research Station and CLYTIE [14] and SAFEAIR [15], developed by Thames Polytechnic in London, represent several field models that have been developed specifically for fire scenarios.

The overall objective of our current research is to develop an advanced computational tool that can be used to assess the damage (and effectiveness of control measures) to the interior compartment of a surface ship / submarine under different scenarios. Such a tool will ultimately predict the firefighting capabilities of any suppressant system in a realistic machinery space environment. Since the geometry of the compartment and its furnishings can have significant effects on the nature of the recirculation patterns, the higher spatial resolution obtained in field modeling techniques is required. In the past, Prasad et. al [16], [17] have used an eulerian sectional water-mist model with gas phase Navier-Stokes equations (field model) for studying mist entrainment and overall suppression of liquid methanol pool fires. The model accurately predicted the suppression and extinction of laboratory scale pool fires and provided a detailed understanding of the relative contribution of the various suppression mechanisms. The computational domain consisted of a stretched 120×128 grid with overall physical dimensions of 9.5×64.0 cm. Typical computational time on a C-90 single processor machine was approximately 10 hours. If this approach is used directly to model realistic 3-D fires in large complex enclosures (such as the ex-USS Shadwell), the CPU costs and memory requirements will be prohibitive.

In this report we first describe the method of domain decomposition based on the multiblock "CHIMERA" approach [18] to solve the unsteady compressible Navier-Stokes equations inside a large fire compartment. The advantages of using the multiblock approach over conventional techniques for simulating large scale fires is discussed. Parallel implementation of the mathematical models is outlined. Computations are performed to demonstrate seamless fluid flow through three embedded grids. Communication between the grids, hole construction and overlapping of the grids is discussed in detail. Then, we describe simulations for a 330 kW and a 980 kW fire in a single uncluttered fire compartment and show comparisons with experimental data. Computations were also performed to simulate a 1310 kW fire in a multi-compartment geometry that replicates the ex-USS Shadwell. Velocity vectors and temperature profiles provide a detailed understanding of the complex flow field and vortical structures that evolve within the ship compartment. These tests serve as a demonstration of our capability to simulate fires and smoke spread in a large multi-compartment enclosure.

2. PROBLEM FORMULATION

Several recent developments in computational techniques have been combined to develop a tool that can be used to simulate fires in large complex enclosures. The main obstacle in solving the reactive flow field inside a complex ship compartment is the difficulty in efficiently and accurately representing and solving for all the length and time scales of interest. Generating computational

meshes with the required degree of point clustering in regions of interest is a challenging task. It is also desirable to keep the region that requires a mesh to a simple topology that is easy to modify. In addition, a single mesh that is fine enough to resolve the desired features of a complex flow field will be too large for available computer memory. We have adopted a method of domain decomposition based on the multiblock "CHIMERA" approach [18] which allows a system of relatively simple grids, each describing a component of the complex geometry, to be combined into a composite grid to yield solutions for complex flow fields. The domain decomposition technique subdivides the entire computational region into several smaller blocks. Each block allows a more easily constructed mesh. The Chimera approach requires that adjacent blocks overlap each other in a way that flow field information can be exchanged. Independent blocks communicate flow field information with adjacent blocks through a system of artificial boundaries also known as interpolation boundaries and hole creation boundaries.

In a typical fire compartment problem we will find a number of small fires at various locations in an enclosure. Such a problem can be solved using the multiblock technique by constructing several finely resolved meshes embedded in a coarser mesh. The finely resolved blocks solve for the detailed flow field around the individual fires, whereas the coarsly resolved block solves for the convection of hot gases and smoke through the larger fire compartment itself. Another advantage of the multiblock technique is that different physical processes (governing equations) can be solved for in the different blocks. For example, in the finely resolved blocks around the fire, we may solve for the multi-component chemically reacting fluid flow as well as the diffusion and transport of the various species, while in the larger coarser blocks, we could solve only for the transport of smoke and hot gases. Besides using different sets of governing equations in the various blocks, different numerical integrators can be employed. For example, explicit integrators may be employed in the larger coarser blocks and implicit reaction kinetic integrators can be used in the finely resolved blocks. The multiblock Chimera approach also results in grid cells with aspect ratio closer to unity as compared to other approaches such as non-uniform gridding techniques which may give rise to highly skewed grids. Fractional time step splitting techniques are used not only for the physical processes but also to couple the solutions for the individual blocks. The presence of obstacles in the fire compartment can also be simulated using the domain decomposition technique by constructing holes in the meshes at the appropriate locations. These techniques can be tailored for each problem so as to resolve the time and length scales of interest.

Application of the Chimera scheme requires two steps: 1) a description of how each mesh is to communicate flow field information to other meshes, and 2) execution of a flow solver that uses the communication information generated in step 1. Step 1 is performed by a code named PEGSUS [19] which determines the boundary points in a mesh which must be updated by interpolated flow variables from other meshes and calculates the required interpolation coefficients for these mesh points. In step 2, the composite mesh and the interpolation file are input into the flow solver. The Navier-Stokes equations for conservation of mass, momentum and energy [16], [17] are employed to model the growth and spread of a fire through a three-dimensional geometry.

$$\frac{\partial \rho}{\partial t} + \frac{\partial (\rho u)}{\partial x} + \frac{\partial (\rho v)}{\partial y} = 0, \tag{1}$$

$$\frac{\partial (\rho u)}{\partial t} + \frac{\partial (\rho u^2 + P)}{\partial x} + \frac{\partial (\rho uv)}{\partial y} + \frac{\partial (\rho uw)}{\partial z} = 0, \tag{2}$$

$$\frac{\partial(\rho v)}{\partial t} + \frac{\partial(\rho vu)}{\partial x} + \frac{\partial(\rho v^2 + P)}{\partial y} + \frac{\partial(\rho vw)}{\partial z} = -\rho g, \tag{3}$$

$$\frac{\partial(\rho w)}{\partial t} + \frac{\partial(\rho wu)}{\partial x} + \frac{\partial(\rho wv)}{\partial y} + \frac{\partial(\rho w^2 + P)}{\partial z} = 0. \tag{4}$$

$$\frac{\partial(\rho E)}{\partial t} + \frac{\partial(\rho E + P)u}{\partial x} + \frac{\partial(\rho E + P)v}{\partial y} + \frac{\partial(\rho E + P)w}{\partial z} = \frac{\partial q_x}{\partial x} + \frac{\partial q_y}{\partial y} + \frac{\partial q_z}{\partial z} - \rho g v. \tag{5}$$

In these equations x, y and z denote the independent spatial coordinate and t denotes the temporal coordinate; ρ the mass density; u, v and w are the x, y and z components of the fluid bulk velocity; P, the pressure; E, the total energy per unit mass; g, the gravitational body force per unit mass. Constant value for thermal conductivity and viscosity is used. Chemical reactions between the fuel and oxidizer are simulated as a point exothermic energy release process. Fuel flow rates are obtained from experimental data and are combined with thermodynamic values for heat of reaction for complete combustion. This representation was restricted to a single finely gridded block surrounding the immediate vicinity of the fire.

2.1 Numerical Techniques

Explicit algorithms that treat the sharp discontinuities present in fires are extremely inefficient at the low flow velocities associated with fires. The Barely Implicit Correction Flux Corrected Transport (BIC-FCT) algorithm [20], used in the current fire model, combines an explicit high order, nonlinear FCT method [21] with an implicit correction process. This combination maintains the high-order accuracy and monotonicity of FCT but removes the timestep limit imposed by the speed of sound. By using FCT for the explicit step, BIC-FCT is accurate enough to compute the sharp gradients without overshoots and undershoots. These spurious numerical oscillations can otherwise lead to unphysical results.

For use with Chimera techniques, the BIC-FCT method must be slightly modified to take into account those points on the mesh for which the data is interpolated from another block. The IBLANK array, generated by PEGSUS, is used for this purpose. The IBLANK array consists of ones's ("1") and zero's ("0"). A mesh point with an IBLANK array value of "0" denotes a point that is not to be computed on this mesh. These blanked points can be points that are either interpolated from other blocks, or may be points that are out of the computational domain (perhaps lying within a solid body).

The BIC-FCT algorithm is split into two stages. In the first stage, explicit convection with FCT is performed. In this implementation, direction-split FCT is used and each of the three directions (for a 3-D mesh) is advanced in turn. This involves copying the old timestep values into a one-dimensional pencil, advancing the solution with FCT, and writing the new timestep values back from the one-dimensional pencil. It is at this step that the IBLANK array is used. The new timestep values are not updated for any blanked point (where the IBLANK array contains a "0"). Thus for these points, the old timestep values (for the independent and dependent variables) remain unchanged. This modification to the explicit phase is extremely simple, and does not require any modification to the FCT subroutine itself, only to the driver subroutine.

In the second phase, an implicit pressure correction is performed. An elliptical equation must be solved that estimates the pressure at the new time step. The solution procedure for this elliptical equation was modified to take into account the blanked points. For the blanked points (IBLANK array value of "0"), the right hand side of the equation was set to the old timestep pressure, the diagonal element of the coefficient matrix was set to one, and the off-diagonal elements were set to zero. This ensured that the pressure in the blanked points remains unchanged from the old timestep value. After the new timestep pressure is obtained in this domain, the pressure gradient term must be added to the momentum equation which was advanced explicitly by FCT without this term. This term is not applied to the blanked points, thus leaving the momentum in these points unchanged from the old timestep value. The old timestep values of momentum and energy are not updated for the blanked points, in the viscous and thermal conduction modules.

Each block contains cells of different sizes, and thus a different timestep is possible for each block. It would be extremely inefficient if the overall timestep in the calculation were to be limited to smallest of the timesteps. Therefore, the overall timestep is set to the largest, and subcycling is performed on those blocks that require a smaller timestep. The number of subcycles should not be excessive (≤ 50), however. For each block, the solution is advanced as many subcycles as is required to reach the overall timestep. Each governing equation is solved in parallel across the grid points with each block processed sequentially. After all blocks are advanced to the new overall timestep, data is interpolated between the blocks as specified by PEGSUS.

The key feature of the Chimera scheme is that blocks need not be aligned perfectly. This provides the flexibility needed to grid complex configurations (interior of a ship geometry). However, this implies that data transfer is not a simple copy operation but instead, interpolation is needed. The PEGSUS program generates a list of points that are to be interpolated, and assumes that the data for these points will be obtained by tri-linear interpolation from some other block. PEGSUS also indicates the corresponding cells in the other meshes for interpolation (interpolation stencil) and the interpolation coefficients. These lists (output from PEGSUS) are designed for in-core / out-core calculations, where only one block is in memory at a time. For today's computers with adequate memory, this scheme is clumsy and inefficient. In the current code, all blocks are in memory, and the inter-block communication can be turned into a simple gather-scatter operation. The PEGSUS data files are preprocessed before the code is run and a list of points to be interpolated and the location from which the data is to be interpolated is written out. This file contains the indirection arrays for the gather-scatter operation.

Tri-linear interpolation introduces errors into the solution. Since the interblock communication is performed through interpolation, conservation cannot be guaranteed across the blocks. It is not necessary to interpolate only on the independent variables, since strict conservation is not possible. Infact, in the current code the velocities, total density, pressure and species densities are interpolated. The choice of variables was suggested by Edwards [22]. The errors associated with the interpolation process can be kept quite small by proper choice of the meshes. This can be accomplished by ensuring that the size of the cells in the overlap region does not vary greatly between the blocks. A factor of two or less change in cell size ensures a reasonably smooth transition. The lack of smoothness in the transition (from one block to another) is not due to the interpolation, but from the abrupt change in cell size itself. All schemes with mesh refinement face this difficulty. Therefore it becomes important to locate the block overlaps away from regions with high gradients.

2.2 Programming Strategies

The Chimera technique lends itself to a very modular style of programming. Each domain can be treated in similar fashion and subroutines that implement physical models, deal with just one domain at a time. Thus, given a suitable framework it is very easy to convert an existing single domain model to one suitable for use in Chimera methods. One of the key features of the current code is this framework. The framework handles data storage for all domains, provides utilities for a domain to access its data in an extremely transparent manner, and manages the inter-domain communication and data interpolation. Routines are provided for I/O and plotting output. The plotting output is in PLOT3D format and can be read by a variety of CFD graphics packages such as FAST, FIELDVIEW or EnSight.

The framework of the present code is highly flexible to be able to deal with an arbitrary number of blocks each with an arbitrary number of grid points. Even the interconnection between the blocks is arbitrary. Thus the number and size of the objects that must be maintained by the framework is not known a priori. It is extremely wasteful to set a large upper limit on their size or number to accomodate all cases. The framework must dynamically allocate space for domains as required. Fortran 90 was selected as the programming language because it provides this capability among its many object-oriented features. The current code makes extensive use of structures, modules, etc. to both simplify and hide the programming details of the framework from other modules that solve for the physical processes. However, it is still possible to use conventional fortran, thus existing physics modules that are going to be incorporated do not have to be completely rewritten. It was this feature of Fortran 90 that prompted the selection of Fortran 90 over other languages such as C++.

2.3 Parallel Computing

The solution of three-dimensional reactive flow equations on a large number of grid points is a challenging computational task. A simulation of a fire in a complex ship geometry will require tens to hundreds of blocks each with a large number of grid points. This problem is too large for a single processor supercomputer to handle, and so a parallel computer must be employed. In the Chimera framework, parallelization can be performed by framing out the various blocks to different processors. But, since the workload in each block can vary significantly, and there are only a modest number of blocks, load balancing becomes a major problem, and the resulting parallel code will not scale to a large number of processors. The solution to this is to parallelize the individual blocks themselves, and this is the approach taken here. The drawbacks to this approach are that the physics modules have to be individually parallelized and that some blocks may not be large enough to scale properly. However, in the fire model, individual blocks tend to be quite large, so scaling is possible up to a reasonable number of processors.

A code can be parallelized by using message passing or shared memory. Using a message passing library like MPI requires the programmer to explicitly control the work decomposition and manage the information flow. Higher level libraries are available that alleviate some of the burden, but typically extensive modification of the existing code will be required. Shared memory is far easier to use, and in some cases handled automatically by the compiler. However, compilers are unable to detect coarse-grained parallelism present in most codes. In this code, explicit shared memory directives using the OpenMP standard were placed strategically to ensure large regions of

code will operate in parallel. This does require some modification of existing serial code, and may not always be successful. However, shared memory is far easier to use, and can be implemented in stages. The combined choice of Fortran 90 and OpenMP allows this code to be ported to a variety of computers, but it is best suited to shared memory computers such as the Cray C-90 and or the SGI Origin 2000.

3. RESULTS AND DISCUSSION

In this report, three sets of simulations are described to demonstrate the capabilities of the computational tool for improved damage assessment. These are

- Seamless fluid flow
- Fire compartment experiments
- Flow through the ex-USS Shadwell geometry .

These simulations demonstrate our capability to simulate complex flow fields through large enclosures and track the flow of hot gases through complex ship geometries.

3.1 Seamless Fluid Flow

Simulations were performed to demonstrate seamless fluid flow through three overlapping embedded grids. The grids used in the simulation have been shown in Figure 1. "Grid 1" is the finest mesh and is embedded within a coarser mesh "Grid 2". "Grid 2" itself is embedded within the relatively coarser mesh "Grid 3". For the test problem, "Grid 1" is a $32 \times 32 \times 32$ cubic, cartesian mesh with a uniform grid spacing of 10 μm. "Grid 2" is $24 \times 64 \times 24$ cartesian mesh with a uniform grid spacing of 21 μm. Finally, "Grid 3" which is the coarsest mesh used in these simulations is a $24 \times 64 \times 24$ cartesian mesh with a uniform grid spacing of 43 μm. The overall dimension of the computational domain were 1011, 2731 and 1011 μm in the x, y and z directions respectively.

Fresh fluid enters the computational domain through the lower edge of the computational domain in all the three meshes. Inflow boundary conditions are specified at these edges. Fluid leaves the computational domain through the upper edge in "Grid 3". For "Grid 3" both the right and left edges are treated as slip walls. For "Grid 1" and "Grid 2", only the left edge is treated as a slip wall.

Figures 1 and 2 also show the cells that are communicating flow field information across the meshes. "Grid 1" obtains flow information from "Grid 2" at the top and the right edge. The cell locations in "Grid 1" that are accepting flow field information from "Grid 2" have been shaded orange. The cells in "Grid 2" that are sending information to "Grid 1" have been shaded blue. Similarly "Grid 2" obtains flow information from "Grid 3" at the top edge and the right edge. The cell locations in "Grid 2" that are accepting flow field information from "Grid 3" have been shaded green and the cell locations in "Grid 3" that are sending information to "Grid 2" have been shaded blue.

Holes have been cut out from "Grid 2" and "Grid 3" as shown in Figures 1 and 2. The holes are cut out in coarser meshes in regions where the solution is being obtained from the finer meshes. As a result computations will not be duplicated over several meshes at the same point in the computational domain. The construction of holes in the meshes thus results in reduction

in computational costs, but creates hole boundaries which have to be interpolated from other meshes. The hole boundaries in "Grid 2" have been shaded red. "Grid 1" provides flow information (boundary conditions) to "Grid 2" at the hole boundaries. The cells in "Grid 1" that are providing flow field information to "Grid 2" at the hole boundaries have been shaded blue. Similarly "Grid 2" provides flow information to "Grid 3" at the corresponding hole boundaries. The hole boundary in "Grid 3" has been shaded orange and the green cells in "Grid 2" are sending flow field information to "Grid 3".

As discussed earlier, fresh fluid enters the computational domain through the lower edge in all the three meshes. The density of the fluid entering "Grid 1" is half of that which is entering "Grid 2" and "Grid 3". This results in a temperature gradient (since the pressures are the same) between the fluids entering the computational domain. Figure 3 shows the composite mesh that is generated by combining the three meshes. The overlap region between the meshes is also quite evident in this figure. Simulations were conducted to study evolution of a hot square jet through this three dimensional composite mesh. Figure 3 shows the velocity vectors and the temperature contours illustrating the seamless nature of the fluid flow through the three composite meshes. The velocity vectors have been color coded with red showing the highest density and blue showing the lowest density. Results were compared with computations on a single finely resolved mesh. The velocity vectors and temperature contours computed, match very well for the two cases demonstrating our capability to simulate fluid flow through overlapping and embedded meshes without losing accuracy. This simulation serves as a demonstration of our capability to simulate fluid flow through three overlapping, embedded meshes in a seamless fashion.

3.2 Fire Compartment Experiments

Dembsey, Pagni and Williamson [23] have performed a set of full-scale compartment fire experiments suitable for model comparison. The experiments were conducted in a fire test compartment (Figure 4) which is 2.5×3.7 m in plan and 2.5 m in height. The compartment is similar in size, geometry and construction to the standard fire test compartment specified in Uniform Building Code Standard 8-2. A 0.61 $m \times$ 1.22 m porous surface burner was placed in the center of the compartment. The burners porous surface was 0.61 m above the floor of the compartment. Propane fuel was supplied at a steady rate to obtain a 330 kW or 980 kW fire for the duration of each experiment. As shown in Figure 4, the ceiling gas temperature distribution was measured using fifteen thermocouples arranged in a uniform grid centered in the compartment, 0.10 m below the ceiling.

The compartment has a single doorway, 0.76 m wide $\times 2.0$ m high centered on one of the shorter sides. Any computational mesh that is restricted to the fire compartment would require prescription of boundary conditions at the door. The flow field through the door is not known a priori. As our simulations will show, portions of the door are an inflow boundary while other parts of the door are outflow boundaries. We also observe that as vortical structures continuously flow through the door, the flow field at the door is time-dependent in nature. As a result it is very difficult to prescribe any boundary conditions at the door. We have used three embedded meshes to simulate the burner, the fire compartment and the flow field through the door (Figure 5) into a large outer compartment. The details of the geometry outside the doorway in the experiments were not available.

The fire compartment is gridded with a $36 \times 24 \times 24$ cartesian mesh with a uniform gridding of

10.0 cm. The burner and the fire are gridded relatively finely using a $32 \times 24 \times 24$ cartesian mesh embedded within the fire compartment mesh. The fire compartment is connected through the door to a very huge compartment referred to as the "outer compartment". The outer compartment is gridded with a $64 \times 48 \times 72$ mesh. The presence of the outer compartment does not appreciably increase the cost of the calculations, but it provides a reasonable way of computing the flow field through the door. The door now becomes an interior plane of the computational domain and not a boundary condition.

Simulations were performed for a 330 kW fire located in the center of the compartment. The fire was ignited at $t = 0$ s and the simulations were terminated at $t = 1800$ s. Figure 6 shows instantaneous streaklines at $t = 1800$ s in the fire compartment. The streaklines have been color coded with temperature, with red showing the highest temperature and blue showing the lowest temperature. The edges of the fire compartment, fine mesh in the burner and the flow of hot gases through the door are all shown in the figure. The streakline pattern clearly illustrates that large scale vortical structures are continuously evolving in the fire compartment and are convecting through the computational domain.

Figure 7 shows instantaneous velocity vectors at two different sections. The sections are taken at different distances (1.25 and 1.50 m) from the right wall (darkest wall in Figures 5 and 6). Both sections are parallel to the right wall. The velocity vectors have been color coded with blue showing the lowest temperature and red showing the highest temperature. The section at 1.25 m from the right wall passes through the center of the compartment and shows the flow field through the door as well as in the burner. Clearly, hot gases are flowing out of the fire compartments through the upper half of the door, while cooler air is being entrained into the fire through the lower half of the door. This section also shows the entrainment of the air into the fire plume and the transport of hot gases towards the ceiling. As the plume hits the ceiling, it gives rise to vortical structures, which eventually flow out through the door into the outer compartment. The section at a distance of 1.50 m from the right wall shows that the hot gases are flowing out of the fire compartment at all heights along the door. As new vortical structures continuously evolve and flow through the door, the flowfield through the door is continuously changing. We also observe that the flowfield is not symmetric on either side of the plane of symmetry.

Figure 8 shows comparison between numerical and experimental results for a 330 kW fire. The experimental data (top left figure) is recorded at fifteen thermocouples located 0.1 m below the ceiling (bottom left figure). The maximum steady-state ceiling jet temperature was approximately $401°C$. In general the temperature measured in the rear of the compartment were lower than the temperatures measured in the front. The instantaneous data from the numerical simulations has been shown in Figure 8 (top right figure) at 1800 s into the simulations. When the fire is ignited, there is an initial transient, during which the temperature in the compartment increases from room temperature to a value close to $350 - 400°C$. However as air is continuously entrained into the fire, new vortical structures evolve and flow through the fire compartment. The presence of these vortical structures result in fluctuations in the instantaneous temperatures. To smooth out these fluctuations, the ceiling jet temperatures were time averaged over a period of 600 *seconds* as shown in Figure 8 (bottom right figure). The time averaged data is more symmetric and compares fairly well with the experimental data.

Simulations were also performed with a 980 kW fire (Figure 9) in a single uncluttered fire compartment. Figure 9 (top left) shows experimental data recorded at the 15 thermocouples. The

maximum ceiling jet temperature recorded was approximately 954 ^0C. Experimental data indicates a higher temperature in the region close to the door and lower temperatures in the regions away from the door. Figure 9 (top right) shows numerical results (instantaneous) at 1800 *seconds* after ignition. As in the case of 330 kW fire, the numerical data was time averaged over a period of 600 *seconds*. The time averaged temperature data has been shown in Figure 9 (bottom right). The time averaged data also shows higher temperatures in the front of the compartment (close to the door) and lower temperatures in the back of the compartment. The time temperature history has also been shown in Figure 9 (bottom left). The temperature increases from room temperature to a value close to 900 ^0C. We observe a lot of fluctuations in the temperature data for the first 200 *seconds* after ignition, but the fluctuation intensity reduces after 500 *seconds* into ignition. As the fire size increases the turbulence intensity will also increase. Good turbulence models may improve the quality of the comparison between numerical and experimental data. A better controlled experiment in which the flowfield through the doorway and in the outer compartment is known, will also improve the comparison between numerical and experimental data.

3.3 Flow through the ex-USS Shadwell geometry

The multiblock domain decomposition technique that we have developed is specially suitable for studying reacting flow fields in complex multi-compartment ship geometries. We next discuss simulations performed to understand the movement of hot gases through the various doors and hatches of the ex-USS Shadwell (Figure 10). A closed boat scenario was modeled in which all the external doors and hatches were closed [24]. A system of 17 independent, overlapping rectangular meshes involving 1.2 million grid points (Figure 11) were designed to model the 13 compartments and were coupled together using Pegsus to obtain a composite mesh describing the 9 doors and 8 hatches that connect the various compartments (blocks). The fire was located in the laundry room in a 1.05 m square pan with a diesel fuel mass loss rate of 0.025 kg/s and a heat release rate of 1310 kW.

Figure 12 shows instantaneous temperature contours at a section parallel to the port wall and passing through the center of the ex-USS Shadwell geometry. Our simulations clearly show a hot plume rising from the fire located in the laundry room and the movement of hot gases through the various compartments. The perturbations in temperature are due to the presence of unsteady vortical structures that are observed in the laundry room. Instantaneous velocity vectors (figure 13) and streakline patterns were used to understand the nature of the flowfield established in the ship compartment. These results clearly show the entrainment of air into the fire and the flow of hot gases from the laundry room to the various ship compartments through the doors and hatches. In all the compartments, we observe the presence of large vortical structures that are continuously evolving. As expected, the hot gases accelerate as they flow through the doors or hatches due to area reduction and slow down as they enter larger compartments.

4. CONCLUSIONS

A domain decomposition technique based on the multiblock Chimera approach has been developed to simulate the reactive flow field inside large, complex multi-compartment enclosures. The unsteady form of the compressible Navier-Stokes equations with chemical reactions are solved. The advantages of the multiblock technique over conventional deterministic field models have been discussed. The multiblock technique allows one to construct very fine meshes in and around the fires.

These fine meshes are embedded in a coarser mesh covering the larger fire compartment. This was illustrated by performing simulations for a 330 kW fire and a 980 kW fire with a peak temperature of 430 ^{o}C in a single uncluttered compartment. Computed ceiling jet temperatures were found to compare favorably with experimental data. Adjacent blocks overlap each other and communicate flow field information through artificial boundaries in the multiblock approach. This feature was especially useful for simulating multi-compartment enclosures. Computations in geometries that replicate the ex-USS Shadwell demonstrates our capability to simulate fires and smoke spread in complex enclosures.

5. FUTURE WORK

More detailed simulations will be pursued to model the fire growth and spread in complex ship geometries. Ultimately, simulations of full scale tests of water-mist systems will be conducted in a cluttered machinery space of the ex-USS SHADWELL . These tests will demonstrate the potential ability of water mist to extinguish both shielded and unshielded fires in full scale, relatively cluttered, machinery space applications. Several changes will be made to the present algorithms to simulate machinery spaces. These include improvements to the fire model as well as adding details to the interior of the compartments using the VCE technique [25].

6. ACKNOWLEDGEMENT

The work described in this report was performed by the Laboratory for Computational Physics and Fluid Dynamics of the Materials Science and Component Technology Directorate, Naval Research Laboratory. The work was funded by the Office of Naval Research, Code 334, under the Damage Control Task of the FY-99 BA2 Surface Ship Hull, Mechanical and Electrical Technology Program (PE0602121N) and the NRL 6.1 Computational Physics Task Area. The authors acknowledge Prof. Jack Edwards at North Carolina State University for his help in the early stages of developing the various models discussed in this report.

7. REFERENCES

1. Drysdale, D., *An Introduction to Fire Dynamics*, John Wiley & Sons, New York, 1985.
2. Fowkes, N. D., "A Mechanistic Model of the 1973 and 1974 Bedroom Test Fires," in P. A. Croce, ed., "A Study of Room Fires Development: The Second Full-Scale Bedroom Fire Test of the Home Fire Project," Vol. II, FMRC Tech. Rept., No. 210114, pp. 8-50 (1975).
3. Quintiere, J., "Growth of Fire in Building Compartments," in Robertson, A. F., ed., Fire Standards and Safety, ASTM STP 614, American Soc. for Testing and Materials, pp. 131-167 (1977).
4. Pape, R. and Waterman, T., "Modification to the FIRES Pre-Flashover Room Fire Computer Model," IITRI Project J6400, IIT Res. Inst., Chicago, IL (1977),
5. Mitler, H. E., "The Physical Basis for the Harvard Computer Fire Code," Home Fire Proj. Tech. Rep., No. 34, Harvard Univ., Cambridge , MA (1976).
6. Heckestad, G., *F. Safety J.*, 7:25-32 (1984).
7. Walton, W. D., "ASET-B A Room Fire Program for Personal Computers," National Bureau of Standards," NBSIR 85-3144, Washington, DC (1985).
8. Jones, W. W., "A Multicompartment Model for the Spread of Fires, Smoke and Toxic Gases," F. Safety J., 9, pp.55-79 (1985).
9. Mitler, H. E. and Rockett, J. A., "User's Guide to FIRST, A Comprehensive Single-Room Fire Model," CIB W 14/88/22, National Bureau of Standards, Gaithersburg, MD (1986).
10. Satterfield, D. B. and Barnett, J. R., "User's Guide to WPI-Fire Version-2 (WPI-2)-A Compartment Fire Model," Worcester Polytechnic Institute, Center for Fire Safety Studies, Worcester, MA (1990).
11. Yang, Y. T., Chang, L. C., "UNDSAFE-I: A Computer Code for Buoyant Flow in an enclosure," NBS-GCR-77-84, (1977).
12. Baum, H. R. and Rehm R. G., "Calculations of Three-Dimensional Buoyant Plumes in Enclosures," Combustion Science and Technology, 40, pp. 55-77 (1984).
13. Kumar, S., Hoffman, N. and Coz, G., "Some Validation of JASMINE for Fires in Hospital Wards," Numerical Simulation of Fluid Flow and Heat/Mass Transfer Proesses, Springer-Verlag, Berlin, p.159 (1986).
14. Hoffman, N., Galea, E. R. and Markatos, N. C., "A Computer Simulation of Fire-Sprinkler Interaction: A Two-Phase Phenomena," 12th IMACS World Congress, Paris (1988).
15. Galea, E. R. and Markatos, N. C., "Aircraft Cabin Fires: A Numerical Simulation," 12th IMACS World Congress, Paris (1988).
16. Prasad, K., Li, C. and Kailasanath, K., "Simulation of Water-mist Suppression of Small Scale Methanol Liquid Pool Fires," Fire Safety Journal, 33, pp. 185-212 (1999).
17. Prasad, K., Li, C. and Kailasanath, K., "Optimizing Water-Mist Injection Characteristics for Suppression of Co-Flow Diffusion Flames," 27^{th} Symposium (Int.) on Combustion, pp. 2847-2855, 1998.
18. Steger, J. L., Dougherty, F. C. and Benek, J. A., "A Chimera Grid Scheme," in *Advances in Grid Generation*, ASME FED-Vol. 5, 1983.
19. Suhs, N. E. and Tramel, R. W., " PEGSUS 4.0 Users Manual", AEDC - TR -91 - 8, 1991.

20. Patnaik, G., Guirguis, R. H., Boris, J. P. and Oran, E. S., "A Barely Implicit Correction for Flux-Corrected Transport", J. Comput. Phys., 71:1-20, 1987.

21. Boris, J. P. and Book, D. L., "Flux Corrected Transport I. SHASTA, A Fluid Transport Algorithm That Works,", Journal of Computational Physics, 11 (1) pp. 38-69 (1973).

22. Edwards, J., private communication, (1995).

23. Dembsey, N.A., Pagni, P. J. and Williamson, R. B., "Compartment Fire Experiments: Comparison with Models," Fire Safety Journal, 25 (1995), p.187-227.

24. Williams, F. W., Tatem, P. A., Cummings, W. M. and Scheffey, J. L., "Submarine Firefighting Program Test Plan," NRL Letter Report 6180/0134, 1995.

25. Landsberg, A. M. and Boris, J. P., "The Virtual Cell Embedding Gridding Method: A Simple Approach for Complex Geometries," AIAA Paper No. 97-1982, 1997.

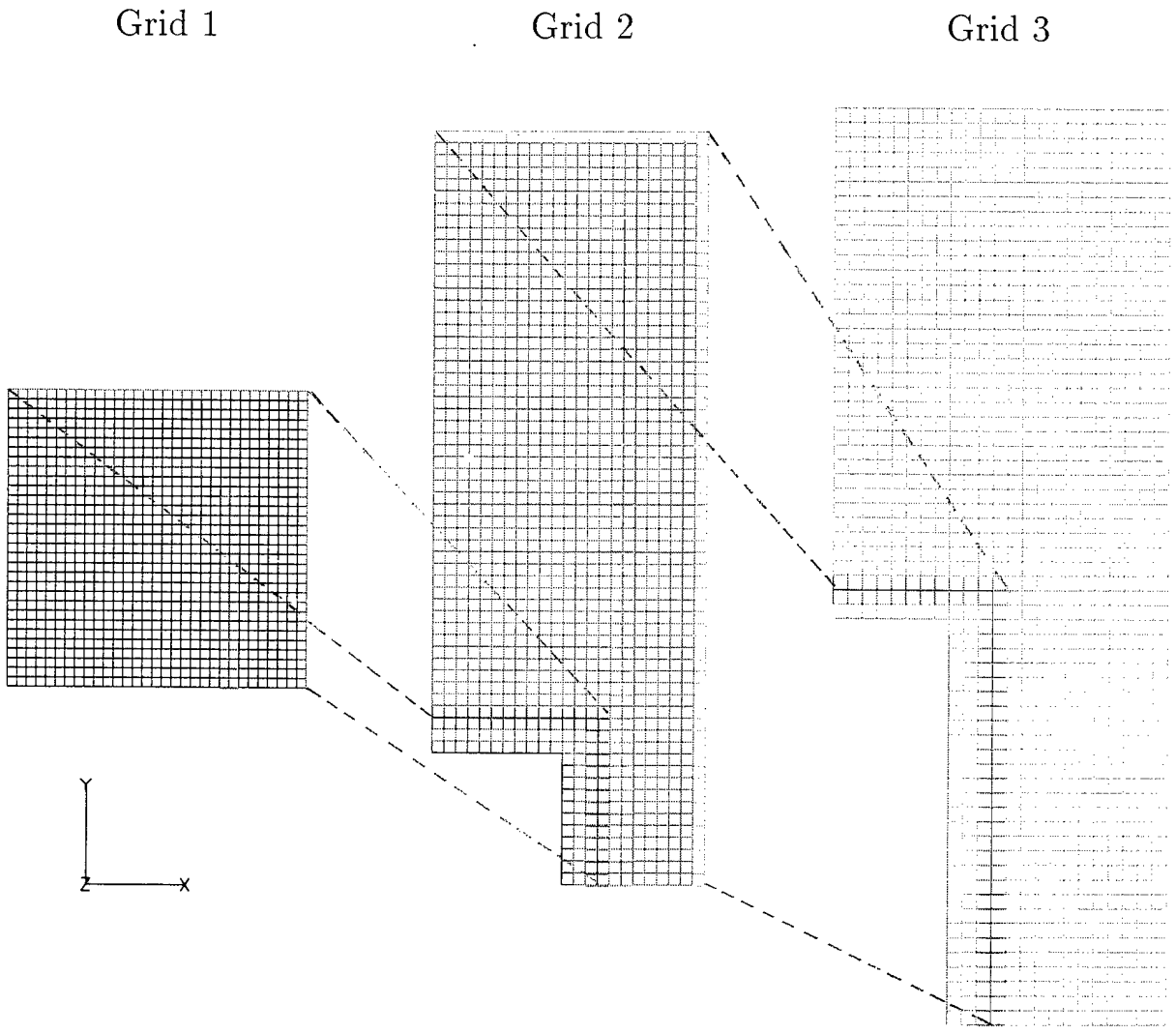

Fig. 1. Three embedded, cartesian meshes used to generate a composite mesh for demonstrating seamless fluid flow of hot gases through a square channel. Also shown are the various artificial boundaries such as hole creation boundaries and the outer boundaries as well as cells used to interpolate flow field information.

Fig. 2. Three embedded, cartesian meshes used to generate a composite mesh for demonstrating seamless fluid flow of hot gases through a square channel. Also shown are the various artificial boundaries such as hole creation boundaries and the outer boundaries as well as cells used to interpolate flow field information.

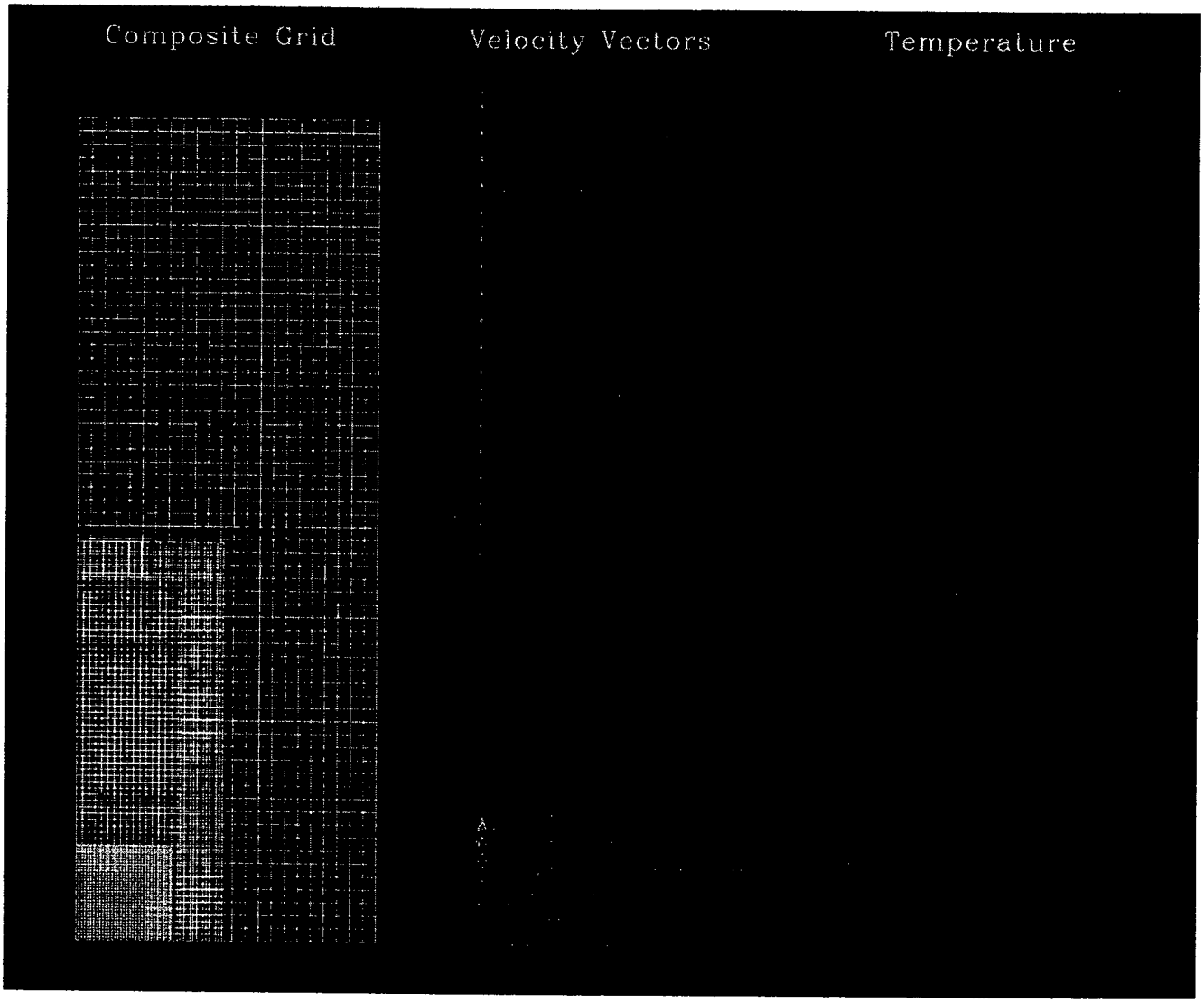

Fig. 3. Composite mesh (left) generated using three independent meshes for simulating seamless fluid flow of hot gases through a square channel in a composite three dimensional mesh. Also shown are the velocity vectors (center) and temperature (right) contours illustrating the seamless nature of the fluid flow through the three overalapping embedded meshes. The velocity vectors have been color coded with temperature and the length of the arrows is proportional to the magnitude of the velocity vectors. Red color indicates a high temperature of 600 ^0K and blue color indicates a low temperature of 300 ^0K.

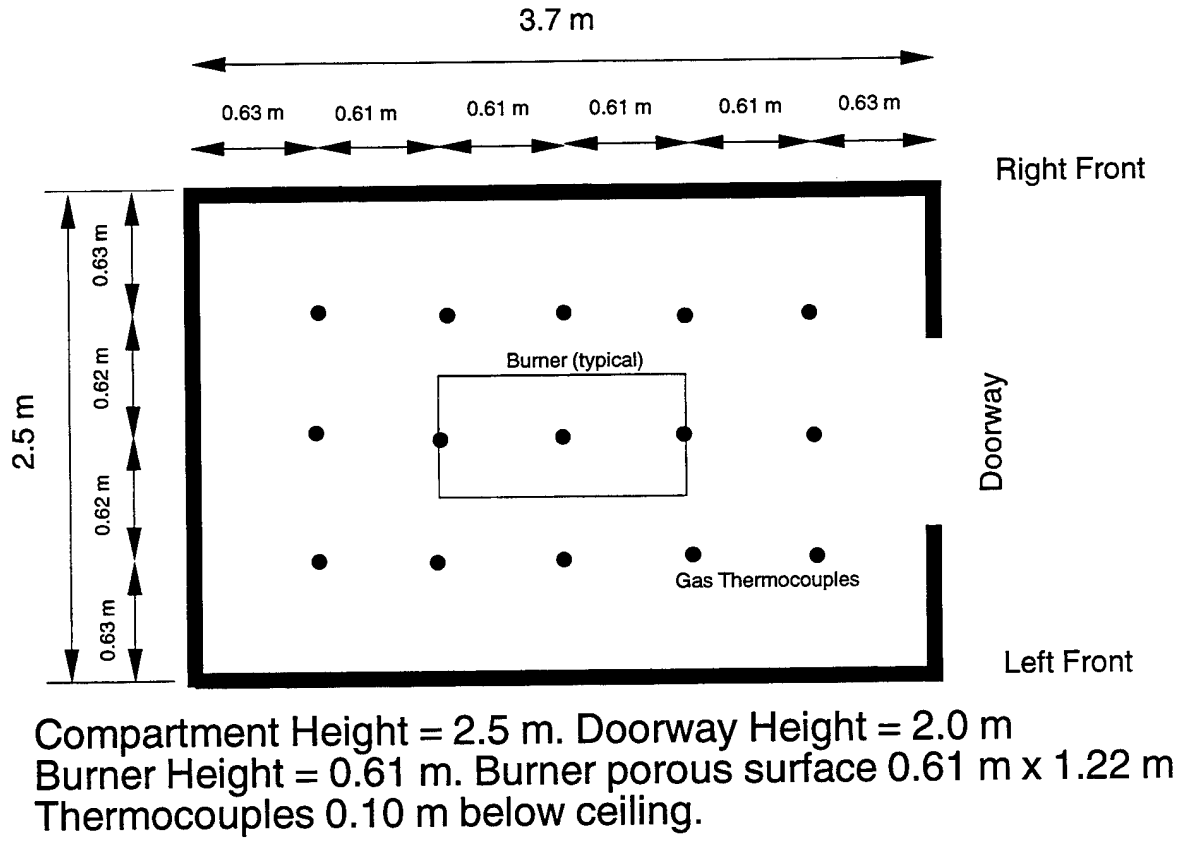

Fig. 4. Fire test compartment plan view (Reference [23]) showing locations of the ceiling gas thermocouples, the burner (located in the center of the compartment) and the doorway.

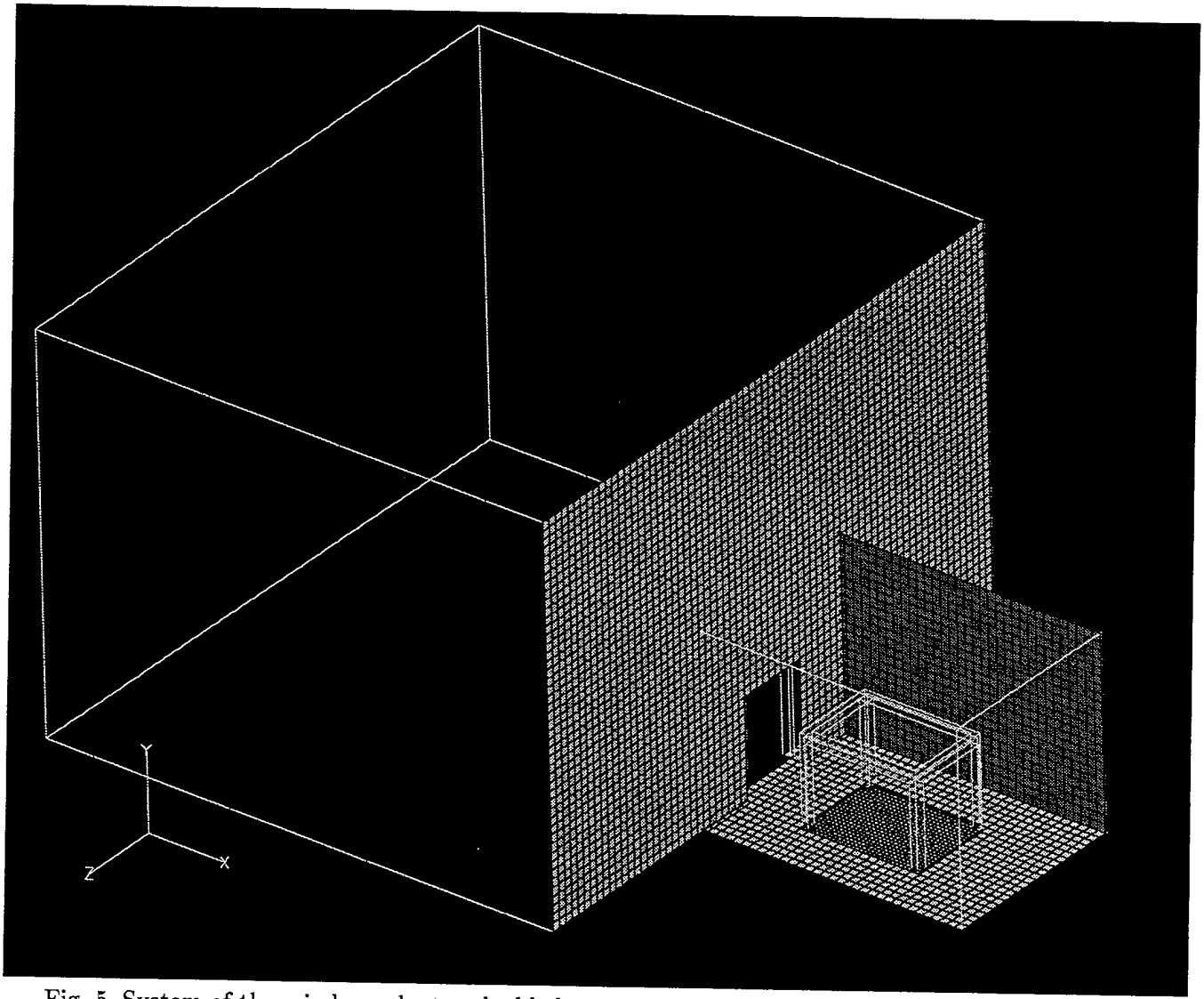

Fig. 5. System of three independent embedded cartesian meshes used to grid the fire compartment, the burner and the outer compartment. Figure shows the mesh surrounding the burner embedded in a coarser mesh covering the fire compartment. The edges of the outer compartment mesh as well as the door connecting the fire compartment with the outer compartment are also shown.

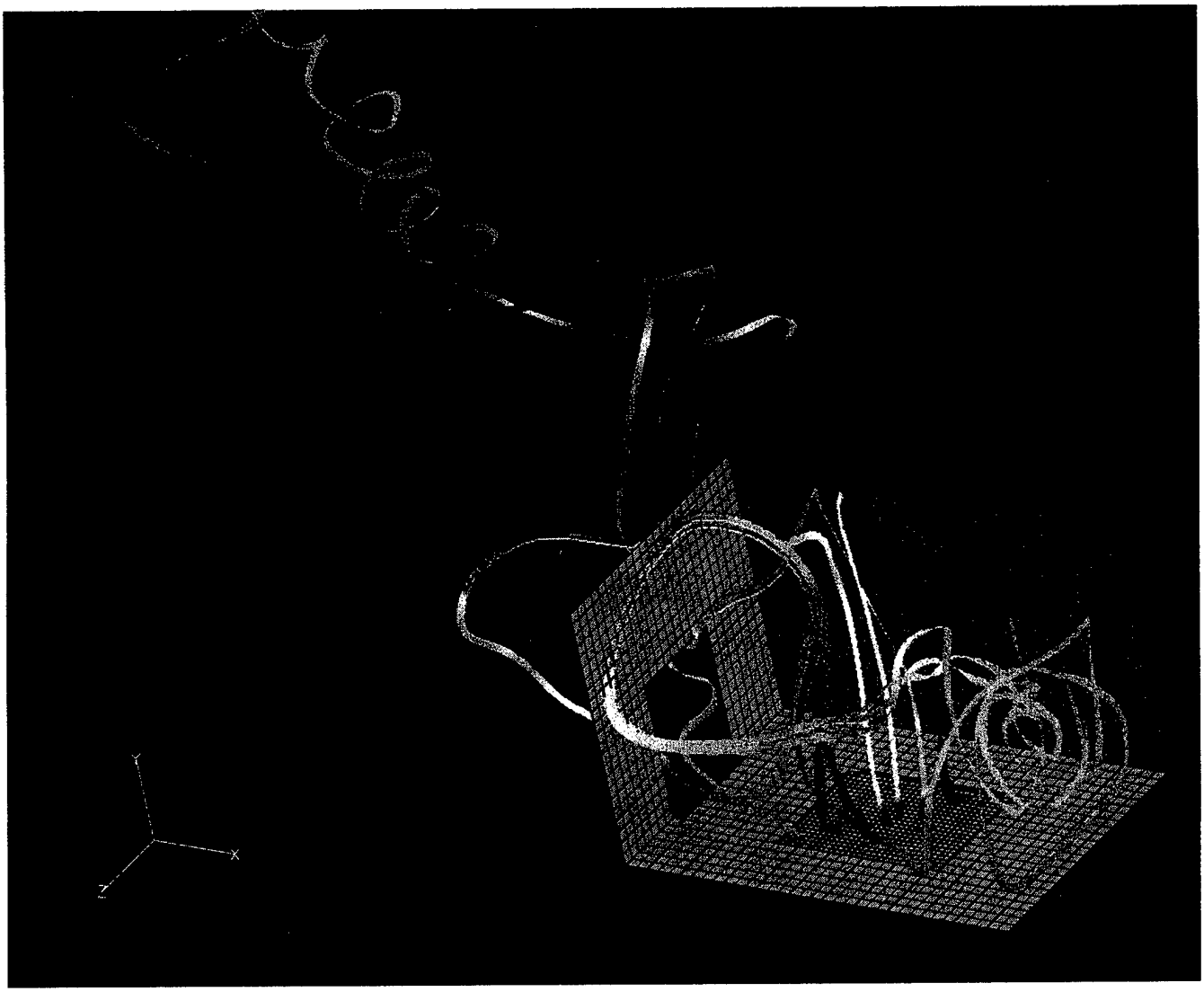

Fig. 6. Streakline pattern in the fire compartment and the surrounding region at 1800 *seconds* after ignition for a 330 kW fire. The streaklines have been color coded with red indicating a high temperature of 400 ^0C and blue indicating a low temperature of 30 ^0C.

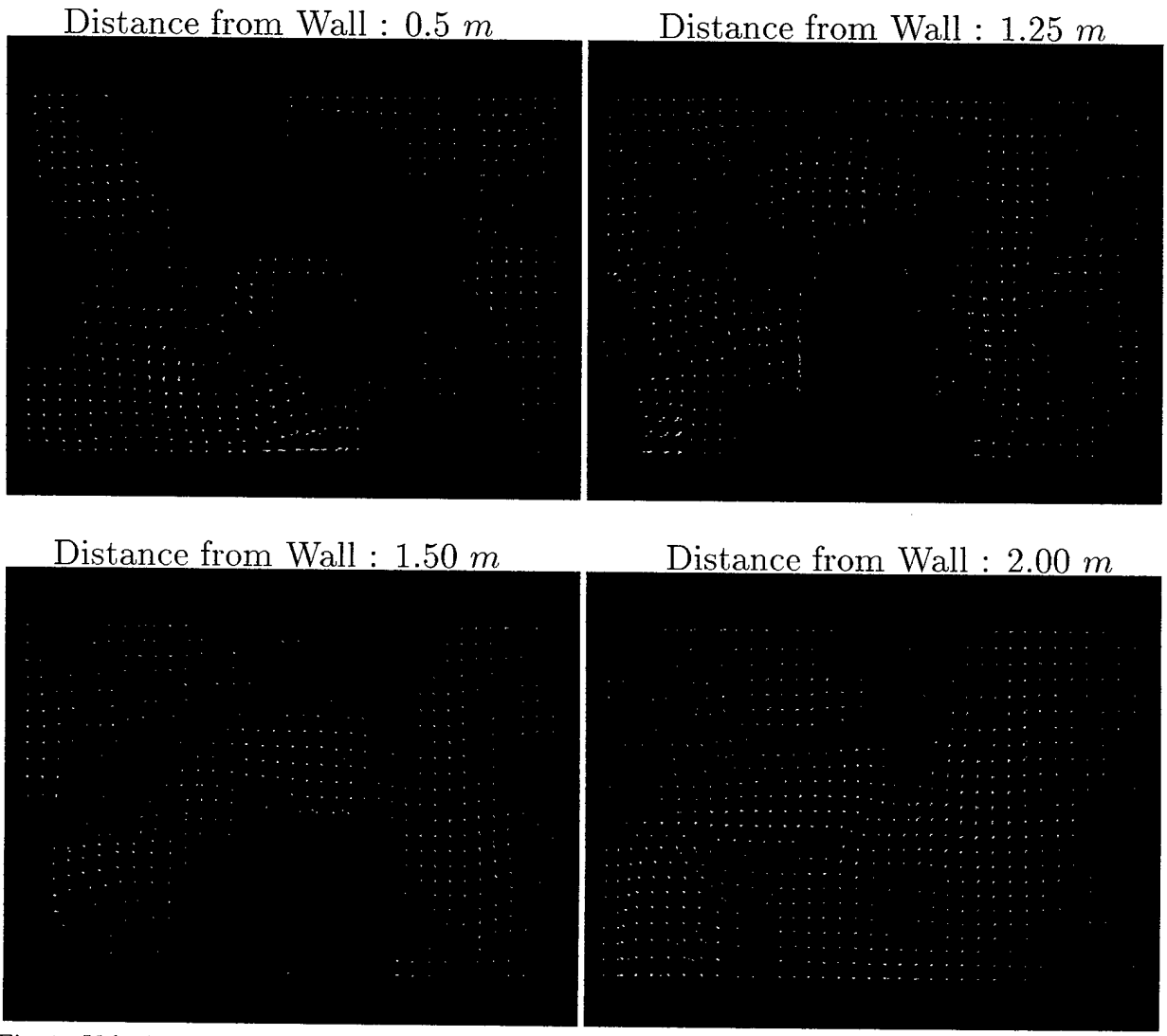

Fig. 7. Velocity vectors in the fire compartment at 1800 *seconds* after ignition for a 330 kW fire. The sections are parallel to the right wall of the fire compartment and are located at a distance of 0.5 m, 1.25 m, 1.50 m and 2.00 m from the right wall. The velocity vectors have been color coded with red indicating a high temperature of 400 ^0C and blue indicating a low temperature of 30 ^0C. The length of the arrows is proportional to the magnitude of the velocity vector.

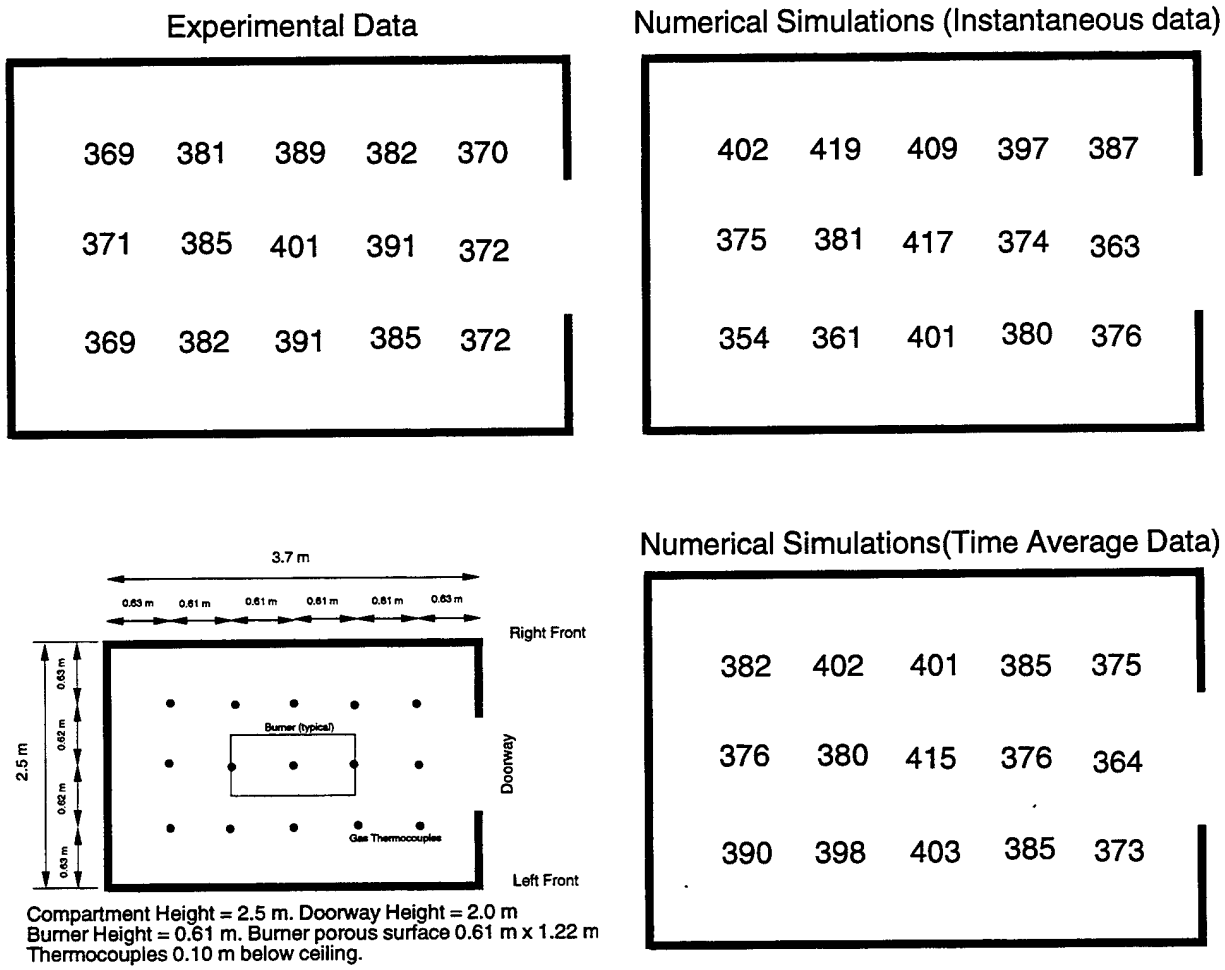

Fig. 8. Experimental data and numerical results of ceiling gas jet temperatures ^{o}C for a 330 kW burner compartment center experiment. Experimental data (top figure) is recorded at 15 thermocouples located 0.10 m below the ceiling. Instantaneous temperature data from numerical simulations (middle figure) is at 1800 *seconds* after the fire is ignited. Time averaged numerical data (bottom figure) is presented by averaging the instantaneous data from 1200 *seconds* to 1800 *seconds*.

Experimental Data

737	778	836	901	887
739	783	857	954	920
742	781	842	903	889

Numerical Simulations (Instantaneous data)

795	796	847	678	783
828	835	854	739	754
693	646	632	713	751

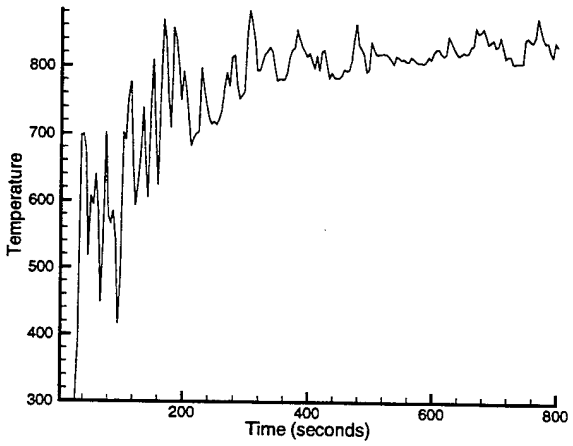

Numerical Simulations(Time Average Data)

785	765	842	788	802
748	805	843	863	823
751	724	803	805	780

Fig. 9. Experimental data and numerical results of ceiling gas jet temperatures ${}^0C$ for a 980 kW burner compartment center experiment. Experimental data (top figure) is recorded at 15 thermocouples located 0.10 m below the ceiling. Instantaneous temperature data from numerical simulations (middle figure) is at 1800 *seconds* after the fire is ignited. Time averaged numerical data (bottom figure) is presented by averaging the instantaneous data from 1200 *seconds* to 1800 *seconds*.

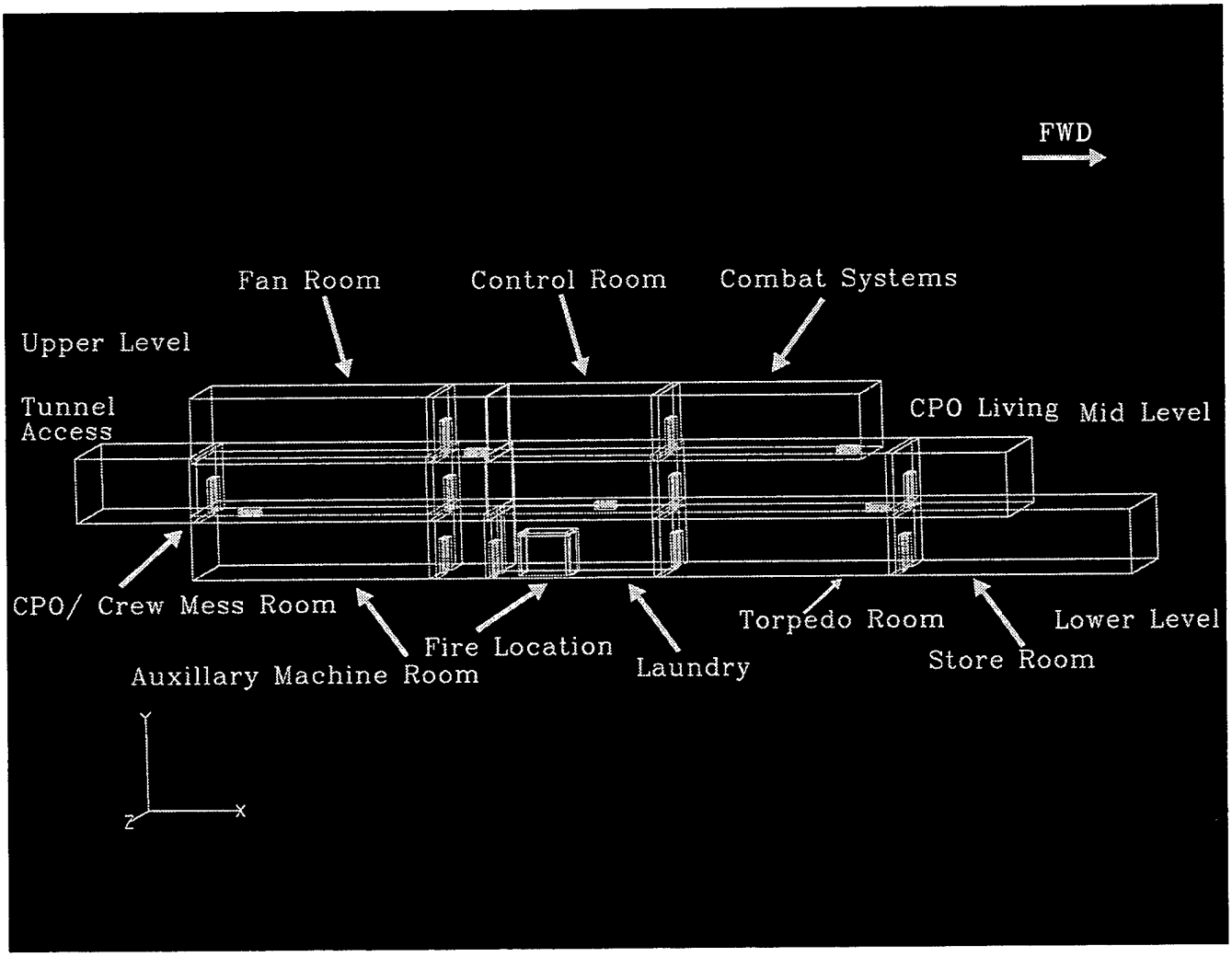

Fig. 10. Isometric view of the SHADWELL/688 test area, as viewed from the well deck.

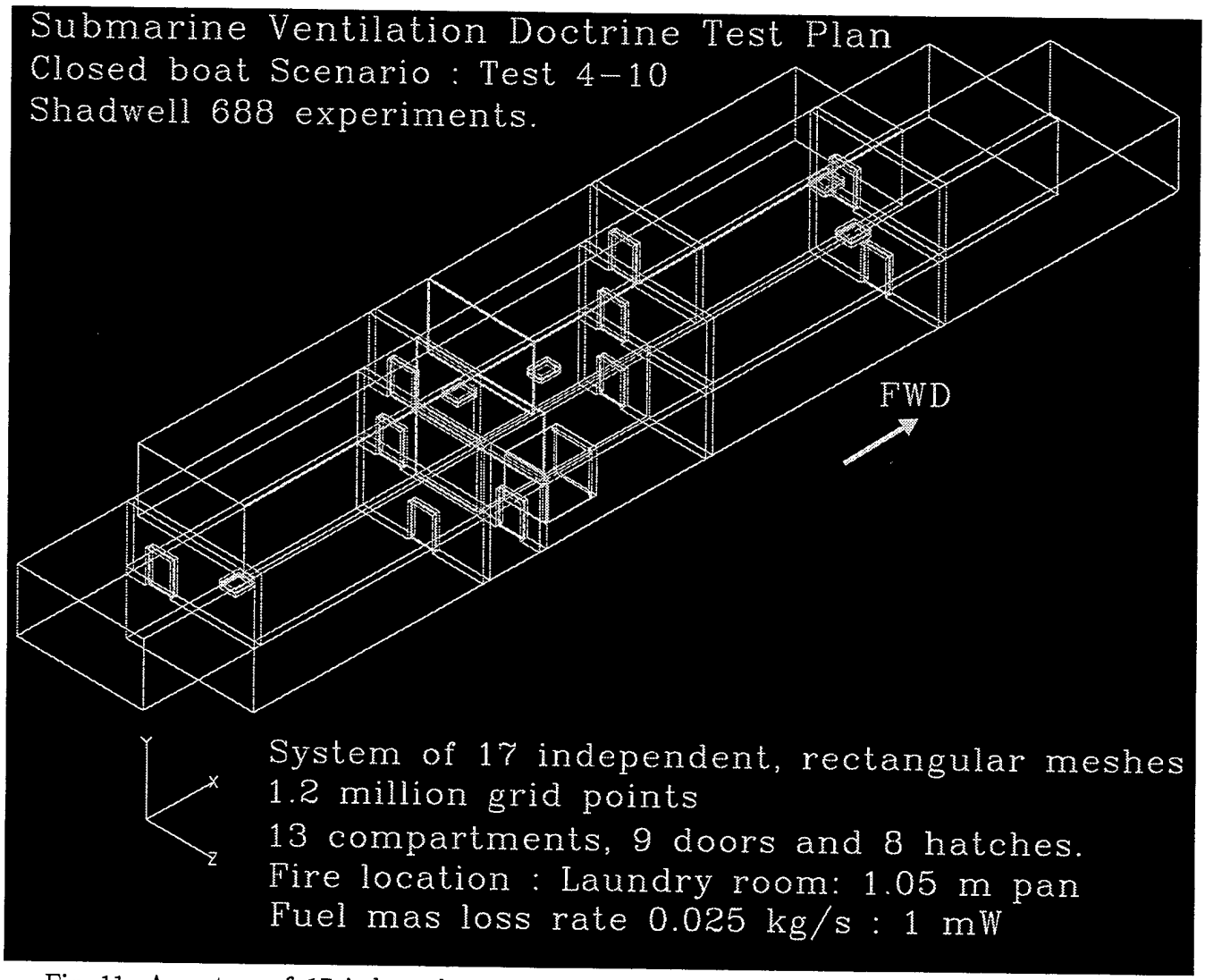

Fig. 11. A system of 17 independent rectangular cartesian meshes were used to grid the 13 compartments as well as the 9 doors and 8 hatches to replicate the ex-USS Shadwell geometry. Figure schematically represents finely resolved blocks embedded in coarser blocks and the overlapping of the individual blocks for exchange of flow field information.

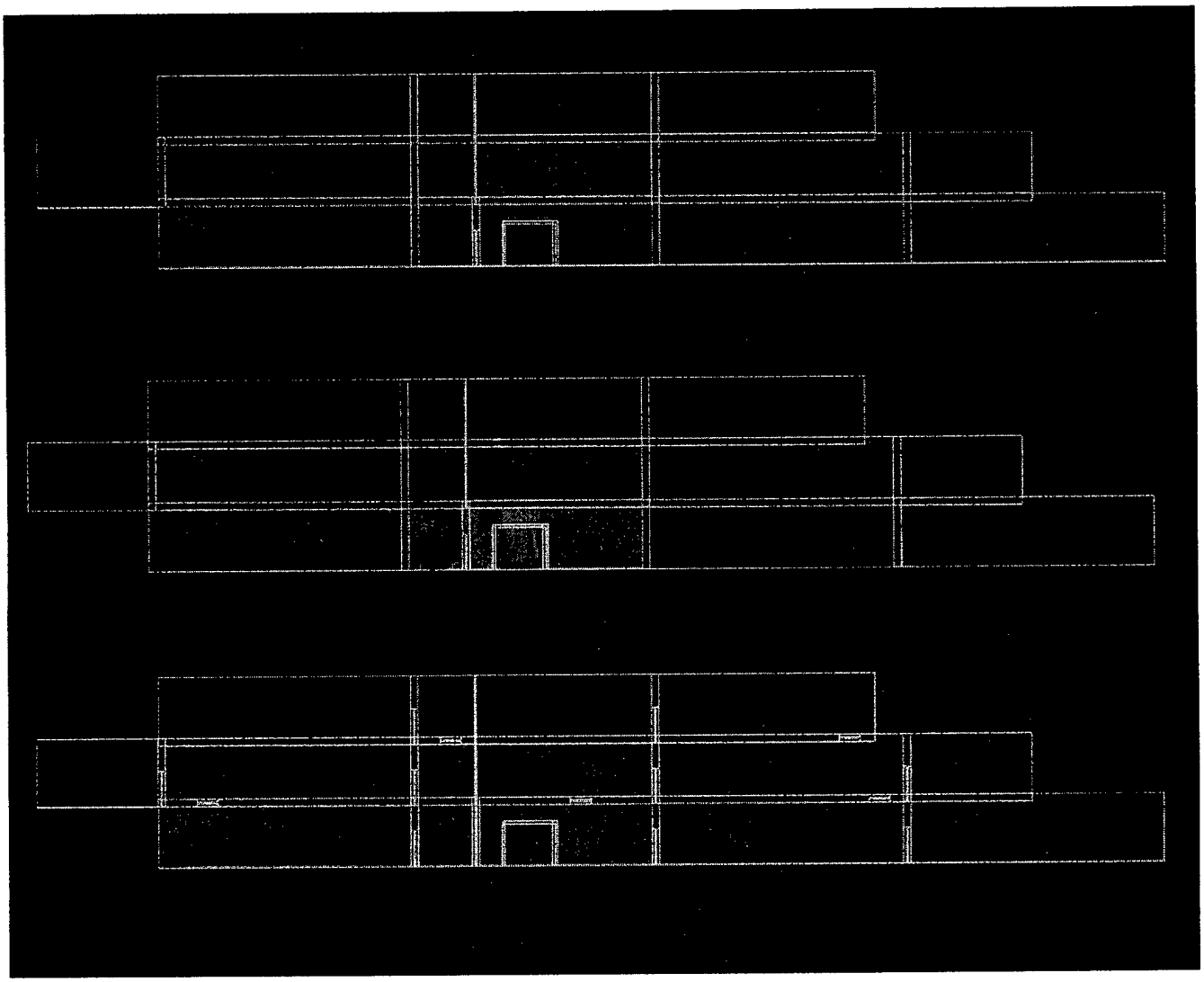

Fig. 12. Instantaneous temperature contours in the multi-compartment ex-USS Shadwell geometry for a 1310 kW fire at 1200 *seconds* after ignition. Red color indicates a peak temperature of 350 ^oC and blue color corresponds to a low temperature of 30 ^oC. The section is taken parallel to the port wall and passes through the center of the ex-USS Shadwell test geometry. The overlapping and embedding of the various blocks has also been schematically represented.

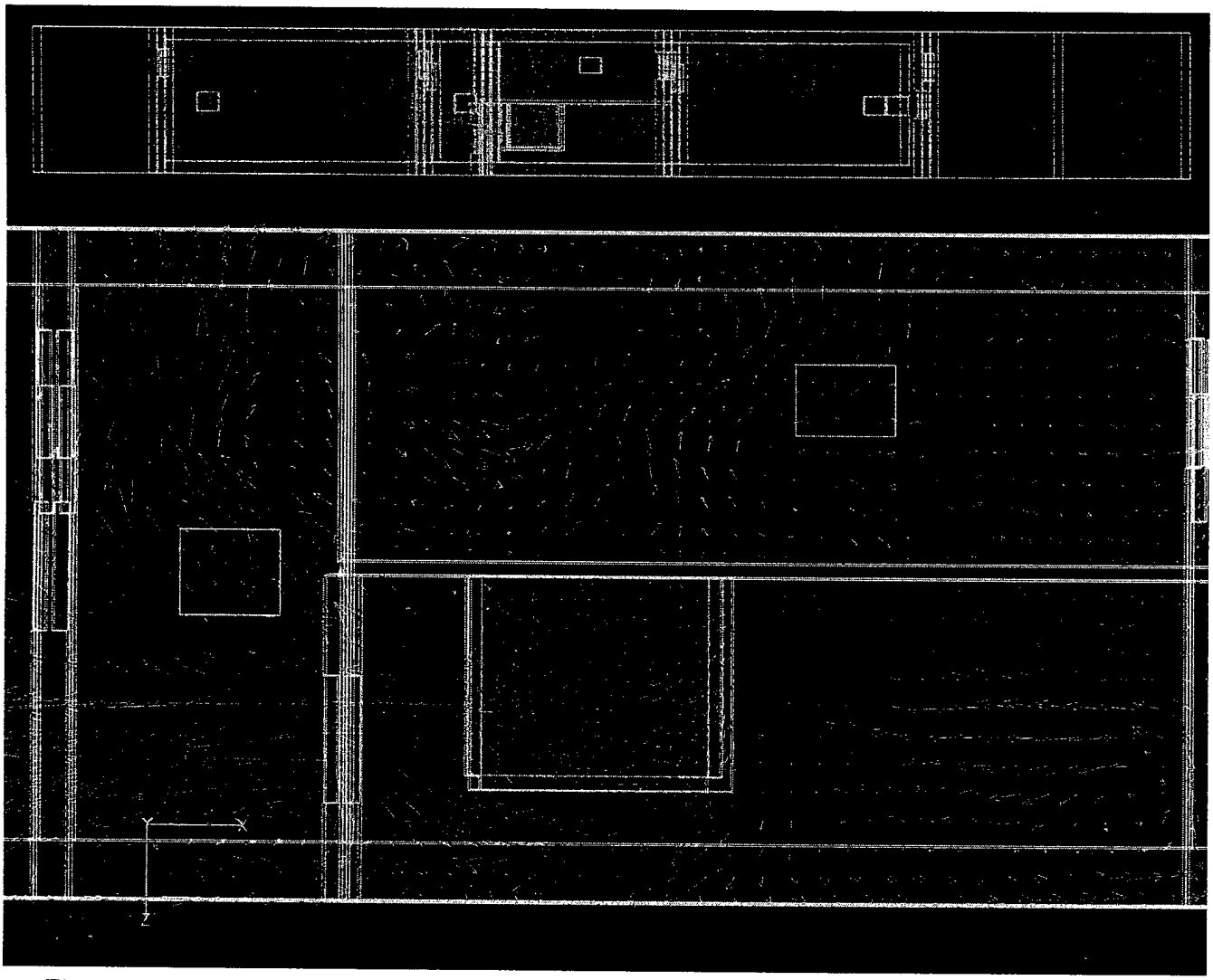

Fig. 13. Instantaneous velocity vectors in the entire lower level of the ex-USS Shadwell geometry (top figure) for a 1310 *kW* fire at 1200 *seconds* after ignition. A detailed view of the laundry room and the laundry room passageway, where the fire is located is also shown (bottom figure), illustrating the flowfield through the doors and hatches. The arrows have been color coded with temperature.